Defence Science Journal, Vol. 66, No. 4, July 2016, pp. 316-322, DOI : 10.14429/dsj.66.10205

REVIEW ARTICLE

Austenitic Oxide Dispersion Strengthened Steels : A Review

Lavanya Raman, Karthick Gothandapani, and B.S. Murty*

Indian Institute of Technology Madras, Chennai - 600 036, India
**E-mail: murty.iitm@gmail.com*

ABSTRACT

Materials play an important role in the fast breeder reactors. Materials used in cladding tube and fuel pins should have better creep and void swelling resistance. To overcome these difficulties, a new class of material known as oxide dispersion strengthened (ODS) steels are used. There are two groups of ODS steels, the ferritic and the austenitic ODS steels based on the matrix. The current status of research in austenitic ODS steels is reviewed. The interaction of dislocations with finely dispersed incoherent, hard particles that governs the strength and high temperature properties of ODS materials is briefly reviewed. The synthesis route adopted for these ODS steels, which is mostly through powder metallurgy route is also discussed. The role of various oxides such as Y_2O_3, $ZrO_2$and $TiO_2$and the clusters formed in these ODS steels on the mechanical properties and void swelling characteristics is also discussed.

Keywords: Cladding tube, ODS steel, oxide dispersion strengthened, powder metallurgy, austenitic

1. INTRODUCTION

Materials that can operate at high temperature, stress with irradiation resistance are needed for advanced nuclear reactors. Ni based super alloys and austenitic steels were considered to be excellent choice of material due to their closely packed structure. Ni base alloys are highly expensive compared to austenitic steels and hence act as a potential materials for the above applications[1-2]. Ferritic and martensitic grades of stainless steel have been used widely in nuclear applications due to their excellent void swelling resistance, but their creep resistance is poor due to their open BCC structure. Austenitic stainless steels have high creep resistance but their void swelling resistance is lower when compared with ferritic steels. The creep and void swelling resistance in austenitic stainless steel can be improved by dispersing ultra-fine stable oxide particles. These oxide particles are expected to reduce grain coarsening and grain boundary sliding and thereby increase the creep resistance and the interface between these oxides and matrix can act as a sink for voids and increases the void swelling resistance in austenitic steels. These steels with oxide dispersions are termed as oxide dispersion strengthened steels (ODS). The evolution of oxide dispersion strengthening in steels has improved both high temperature and irradiation properties. Due to these characteristics of ODS steels, they have been widely studied[2,3].

Austenitic ODS steels are recently developed steels as a candidate for advanced nuclear materials. These steels play vital role in the fourth generation nuclear materials. The high temperature properties and void swelling characteristics are expected to be better than ferritic ODS steels. For more than two decades, ferritic ODS steels have been used in nuclear community and lots of research has been brought out. The Microstructures and composition of nanoclusters, irradiation resistance, and high temperature properties are analysed elaborately. However, the work on austenitic ODS steels is limited. To understand and explain the current status of austenitic based ODS steels, the authors have tried to compile the work done on austenitic ODS steels in this review. Figure 1 shows the number of papers published in austenitic ODS alloys so far, which are not many indicating that the field is still in its infancy.

2. PROCESSING TECHNIQUES OF AUSTENITIC ODS ALLOYS

There are several processing techniques by which austenitic ODS steels can be synthesised. Most of these austenitic ODS steels are produced through powder metallurgy (PM) route. In PM route the powders are prepared by mechanical alloying (MA) and followed by consolidation technique. MA is a solid-state powder processing technique involving repeated welding, fracturing, and rewelding of powder particles in a high-energy ball mill.

Usually hardchrome steels and WC vials and balls are used as milling media during MA. Austenitic ODS steels are made with different grades of austenitic stainless steel like 304[2,4-9], 310[5,10], 316[11–13], 316 L[3] with different percentages of Y_2O_3 and Ti as dispersoids. The MA parameters lie in the range of BPR 5:1 to 10:1, speed 300 RPM - 600 RPM, and MA of these alloys is usually carried out up to 100 hours depending on the milling conditions. The reported consolidation parameters are 50 MPa to 100 MPa pressure with sintering temperature in range of 900 °C - 1100 °C and holding time of about 5 min - 15 min[1-17]. The secondary processing like canning, rolling, forging

Received : 07 May 2016, Revised : 07 June 2016
Accepted : 10 June 2016, Online published : 28 June 2016

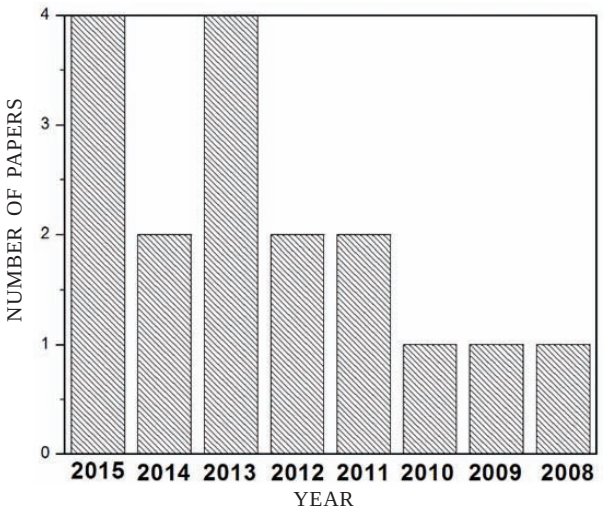

Figure 1. Number of papers on austenitic ODS steels.

or extrusion are carried out after synthesis of ODS steels. The different process parameters are reported based on the secondary processing method. For rolling, the temperature ranges from 1000 °C - 1150 °C whereas, for forging, the temperature ranges from 900 °C - 1150 °C with forging ratio of 3:1[7,13]. The evolution of phases in these steels is studied with respect to milling and consolidation parameters. After processing, BCC and FCC phases are evolved in austenitic ODS steels. Different phases were found to evolve in different grades of austenitic steels. For example, 304 L, and 316 L steel contains mixtures of both FCC and BCC during milling. In case of 310 L steel, it contains only FCC phase after several hours of milling. During the consolidation of 304 L, 310 L, and 316 L steels, they show mixture of both FCC and BCC phase[5]. Yttria and Ti are used as dispersoids in the most of the ODS steels. During milling, yttria dissolves into austenitic phase and further processing (consolidation or heat treatment) of powders leads to formation of nano clusters. Dissolved yttria combines with oxygen and titanium to form complex nano clusters (Y-Ti-O)[1,2,5,7]. Effect of nitrogen dissolution into austenitic ODS steels has also been reported with varying milling time. The morphology of the particles and heat treatment condition for the milled powders are also discussed[6]. Crystallite size decreases and micro strains increase with increase in milling time, as is usually expected. X-ray diffraction analysis shows that the crystalline size and micro strain after milling lie in the range of 9 nm - 11 nm and 0.3 per cent - 0.5 per cent, respectively[1,2]. The parameters used for the synthesis of austenitic ODS steels are given in Table 1.

3. MICROSCOPY OF AUSTENITIC ODS ALLOYS

Austenitic ODS steels normally consist of an austenitic matrix with nano dispersoids. Yttria and titanium are the commonly used dispersoids. The morphology of the pre-alloyed powders changed from spherical to disc shape, after severe collisions during MA. The particle diameter lies in the range of 100 µm to 20 µm[5,7,13]. The microstructure aspects of austenitic ODS steels mainly deals with grain size, morphology and precipitates size and distribution. The grains are relatively equiaxed and the grain size varies from 200 nm to 1 µm[7,13].

The dispersoid size varies from 2 nm to 100 nm[4,7,9,10]. Bimodal distribution of grain size were also reported[7,13]. Dispersoid stend to form after the heat treatment of milled powders. The heat treatment temperature ranges from 550 °C - 1200 °C with different holding time. The heat treatment leads to formation of different phases. Phaniraj[1], *et al*. have reported formation of ɣ-Fe and Al_2O_3 phases at 900 °C for 10 h. ɣ-Fe, Ni_3Fe, $Y_3Al_5O_{12}$ and Y_2O_3 phases evolved during heat treatment at 1100 °C for 24 h Xu[6] *et al*., reported evolution of austenite phases after heat treatment at 900 °C and 1100 °C in presence of nitrogen atmosphere. Wang[5], *et al*., also reported presence of major fraction of ɣ-Fe and small amount of α-Fe. TiN phase formed at 900 °C and $Y_2T_iO_5$ phases formed after 1100 °C. $Cr_{1.36}Fe_{0.52}$and Fe_3Ni_2 were the phases that formed due to the contamination obtained from milling process. The precipitate size and number density of dispersoids increased with heat treatment temperature. At 1200 °C, the precipitate size and number density increased to 15 nm and 10^{-22} m^{-3}, respectively[14]. After heat treatment, the grain size increased from 0.2 µm to 1.8 µm[5,7,13,14]. Oka[14] *et al.* have reported the formation of lamellar structure in austenitic ODS steels and the inter-lamellar spacing decreased with milling time.

4. NATURE OF CLUSTERS : INFLUENCE OF TITANIUM

Precipitation of clusters takes place during heat treatment. Titanium plays a major role in the formation of these nano-clusters. The presence of yttria and titanium tends to form complex nanoclusters in austenitic ODS steels. These complex clusters acts as neutral sink for vacancies and interstitials, thereby improving the void swelling resistance. Different types of clusters formed in ODS alloys are TiN [4,7,8,11], $YAlO_3$ (yttrium aluminum hexagonal (YAH))[11], $YAlO_3$ (yttrium aluminum perovskite (YAP)), $Y_2Ti_2O_7$, Y_2TiO_5, Y_2O_3,$Y_2Hf_2O_7$[1,11,15,16], $Y_2Zr_2O_7$ [14], $Y_2Al_2O_9$ (yttrium aluminum monoclinic (YAM))[4], $Y_5Al_3O_{12}$ (yttrium aluminum garnet (YAG)), Y-Si-Ti-O, Y-Ti-O[1,4,7,8,10]. Y-Ti-O-Al-Ca[9], $Y_2Si_2O_7$, and TiO[3]. Mostly these are Y-Ti-O based clusters. Clusters are normally observed in three different sizes with three different morphologies. They are polyhedral shape with 100 nm, spherical shape with 20 nm - 80 nm and another clusters with size less than 10 nm[4]. Kim[3], *et al*., calculated the minimum free energy change (ΔG) for the formation of precipitates and reported that TiO and $Y_2Si_2O_7$ are the thermodynamically favourable precipitates. The number density of precipitates lies in range of 1.8-3.0 x 10^{22} m^{-3}. The minor additions like hafnium and zirconium tends to increase the number densities of precipitates up to 1 x 10^{23} m^{-3}. Each cluster has its own morphology, size and crystal structure which are given in Table 2.

There are different techniques used to characterise the clusters such as Z contrast mode, high angle annual dark field (HAADF), electron energy loss spectroscopy (EELS) and energy dispersive spectroscopy (EDS)[4,11] attachments in transmission electron microscope (TEM)[1-17], synchrotron X-Ray diffraction and atom probe tomography (APT)[4,11,15]. The APT, EELS, and EDS are used to analysis the chemical composition of the dispersoids. HAADF and selected area diffraction (SAD) are used to analysis structural properties of

Table 1. Synthesis parameters of various austenitic ODS alloys[1-17]

Synthesis	BPR	Time (h)	Speed (RPM)	ODS composition	Sintering parameters			
					Pressure (MPa)	Temp (°C)	Time (h)	Ref.
Ball milling (planetary type ball mill) and Consolidation (HIP)	5:1	30	300	Fe–18Cr–8Ni–1Mo–0.5Ti–0.15Si-0.35Y_2O_3	100	1100	2	1
Ball milling and Consolidation (HIP)	5:1	30	300	Fe-18Cr-8Ni-3Ti-3Y_2O_3, Fe-16Cr-12Ni-3Ti-3Y_2O_3 and Fe-25Cr-20Ni-3Ti-3Y_2O_3	100	1100	2	2
Ball milling (planetary type ball mill)	5:1	24	300	Fe–16.16Cr–13.66Ni-2.33Mo-1.82Mn-0.08Ti- 0.75Si-0.08(Nb+ Ta)-0.05C-0.35Y_2O_3-0.1Ti-0.6Hf	No Consolidation			3
Ball milling (planetary-type ball mill) and Consolidation (HIP)	5:1	30	300	Fe-16.82Cr-13.23Ni-2.4Mo-0.4Mn-0.7Si-0.008C-0.007P-0.005S-0.2N-0.3Ti-0.35Y_2O_3	100	1150	3	4
Ball milling (planetary type ball mill)	5.5:1	96	440	Fe–18Cr–9Ni–2Mn–1Si–0.15S–0.07C-0.35Y_2O_3 and Fe–18Cr–9Ni–2Mn–1Si–0.15S–0.07C- 3Y_2O_3	No Consolidation			5
Ball milling (planetary type ball mill) and Consolidation (HIP)	5:1	30	300	Fe–17Cr–13Ni–2.5Mo–0.7Si–0.4Mn–0.35Y_2O_3–0.5Ti	100	1150	3	6
Ball milling (planetary type ball mill)	10:1	150	380	Fe-18Cr-8Ni-2W-1Ti-0.35Y_2O_3	No Consolidation			7
Ball milling (planetary type ball mill) and Consolidation (HIP)	5:1	30	300	Fe–18Cr–8Ni–1Mo–0.35Y_2O_3– 0.5Ti	100	1100	2	8
Ball milling (Attritor mill) and Consolidation (SPS)	5:1	5	600	Fe-17Cr-12Ni-0.1C-2.5Mo-2Si-1Y_2O_3	50	950	0.08	9
Ball milling (planetary type ball mill)	5:1	30	300	Fe-16.6Cr-13.6Ni-2.33Mo-1.82 Mn-0.08Ti-0.75Si-0.08Nb-0.05C-0.35Y_2O_3	No Consolidation			10
Ball milling (planetary type ball mill) and Consolidation (HIP)	5:1	30	300	Fe–25Cr–20Ni–0.35Y_2O_3–0.5Ti	100	1100	2	11
Ball milling (planetary type ball mill) and Consolidation (HIP)	10:1	60	380	Fe–16.7Cr–8.1Ni–1.1Mo–0.5Ti–0.3Y_2O_3	120	1100	3	12
Ball milling (planetary type ball mill) and Consolidation (HIP)	10:1	60	380	Fe–18Cr–8Ni–2W–1Ti-0.35Y_2O_3	200	1150	3	13
Ball milling (planetary type ball mill)	5.5:1	48	440	Fe-16.6Cr-13.6 Ni-2.33Mo-1.82 Mn-0.08Ti-0.75 Si-0.08Nb-0.05 C-0.35Y_2O_3	No Consolidation			14
Ball milling (planetary type ball mill) and Consolidation (VHP)	10:1	25	300	Fe–18Cr–8Ni–2W and Fe–18Cr–8Ni–2W–0.25Y_2O_3.	200	900	-	15
Ball milling (planetary type ball mill) and Consolidation (HP)	30:1	16	500	Fe–14Cr–20Ni–2.5Mo–2.5Al–2.0Mn–0.5Y_2O_3 and Fe–14Cr–20Ni–2.5Mo–2.5Al–2.0Mn – 5Y_2O_3	50	1100	0.5	16
Ball milling (planetary type ball mill) and Consolidation (HIP)	10:1	12	200	Fe-16.5Cr-11Ni-0.3Ti- 0.3Y_2O_3	103	1150	1	17

the clusters. Miao[11,15], *et al.* has reported the crystal structure, atomic position and coherency of the $Y_2Hf_2O_7$ precipitates with the matrix. The oxide particle exhibits hexagonal structure and shows orientation relationship with the FCC matrix. They have suggested four types of coherency mechanism with respect to orientation and size of the precipitates such as coherency I, coherency II, axis parallel and random orientation. Precipitates with small size (4 nm) have specific orientation with matrix. When the precipitate size increases, it becomes randomly oriented. Among the three non-randomly oriented relationships, axis parallel orientation relationship is the most prevalent. Figure 2 shows a TEM micrograph of the dispersoids in 18 Cr-2W steel[2]. Figure 3 shows APT of clusters in ODS316 steel. The figure indicates that the clusters are Y-Ti-Al-O type[11].

5. MECHANICAL PROPERTIES

The mechanical properties of austenitic ODS alloys are far better than austenitic stainless steels. In austenitic ODS steels the main focus has been on tensile properties and hardness. Mechanical properties are measured both at room temperatures and high temperatures. The yield strength and ultimate tensile strength of the austenitic ODS steels at room temperature ranges from 380 MPa - 852 MPa[3,4,9,11] and 650 MPa - 1000 MPa, respectively[3,4,7,8,10,11]. At 500 °C, the yield strength of these steels ranges from 230 MPa - 440 MPa[3,7,8,10,11]. Similarly, at 700 °C the yield strength ranges from 230 MPa - 300 MPa[3,9].

The percentage of elongation ranges from 25 - 30. The percentage of elongation decreases at high temperatures (500 °C -700 °C) due to the formation sigma phases at these

Table 2. Morphology, crystal structure and size of the clusters in Austenitic ODS steels[1-17]

Clusters	Morphology	Crystal structure	Size (nm)
TiN	Polyhedral	Sodium chloride	100
YAH	spherical	Hexagonal	20-80
YAP	spherical	Perovskite	20-80
$Y_2Ti_2O_7$	-	pyrochlore	<10
Y_2TiO_5	-	orthorhombic	<10
Y_2O_3	spherical	cubic	30
$Y_2Hf_2O_7$	Faceted	Pyrochlore	<10
$Y_2Zr_2O_7$	hexagonal	Pyrochlore	<10
YAM	spherical	Monoclinic	20
YAG	spherical	Cubic	20
$Y_2Si_2O_7$	rectangular	Monoclinic	<400
TiO	spherical	HCP	<400

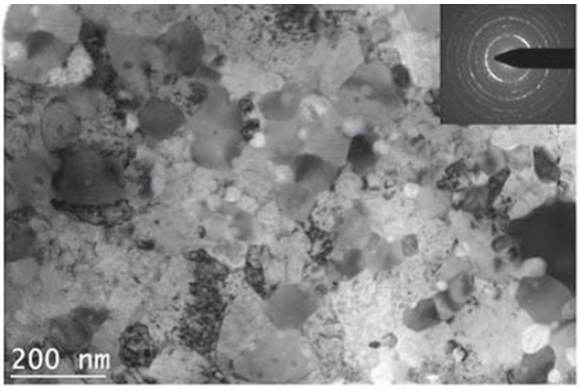

Figure 2. TEM micrograph of dispersoids in 18 Cr-2W alloys[2].

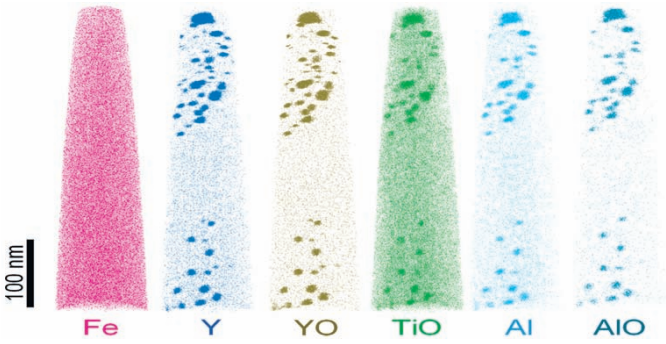

Figure 3. APT results of the ODS 316 steel[11].

temperatures[7]. Figures 4 and 5 shows the variation of tensile properties of various ODS alloys with temperature. The hardness values of ODS alloys ranges from 250 Hv - 300 Hv. The secondary processing of these ODS alloys (rolling and forging) tends to increase the hardness[10]. The tensile properties of these ODS alloys after secondary processing seems to be almost similar[7,10]. *In-situ* synchrotron tensile tests were also carried out in which the load proportioning behavior of matrix and precipitates was estimated. This test showed that finer precipitates like $Y_2Ti_2O_7$ bear more load than other precipitates. They also reported deformation induced martensite formation. The volume fraction and size of these phases were calculated

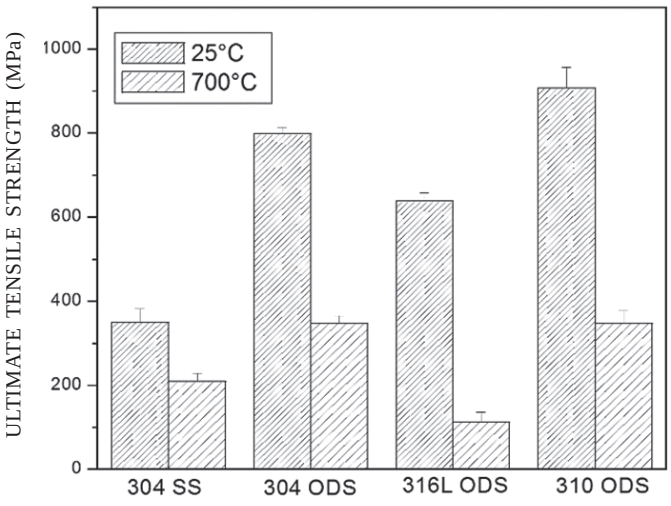

Figure 4. Variation of UTS of austenitic ODS alloys (replotted from[3,7,8,10,16]).

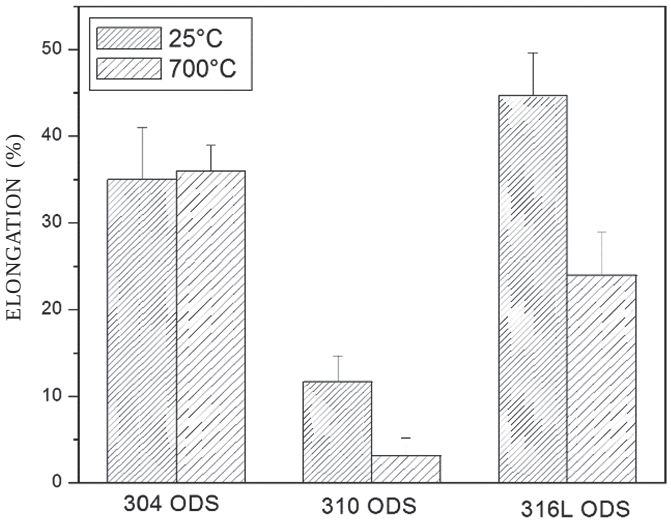

Figure 5. Variation of percentage elongation for various austenitic ODS alloys (replotted from[3,8,10,13]).

in pre tensile and post tensile specimens. Figure 7 shows the variation of *in-situ* tensile test for 310 and 304 ODS steels[4].

A modified Williamson Hall analyses was carried out to understand the dislocation motion in the strained ODS steels. This analysis helps in distinguishing the character of dislocation, dislocation density and ability of twinning or stacking fault formation. At temperatures till 550 °C, the edge character dominates. At higher temperatures, cross slip and dislocation climb are prominent. Based on the activation barrier, either cross slip or climb will dominate[11].

The hardness measured after secondary processing ranges from 275 Hv - 290 Hv. Increase in the hardness is mainly due to decrease of pores size during the secondary processing[7]. The fractographic studies of these ODS alloy have been done to understand the mechanism of the deformation. The dimple and deep structures shows the extent at which plastic deformation takes place and ductile nature of the ODS steel[3,7,8,10].

Oka[14], *et al.* have reported that the presence of minor elements increases the hardness of the Austenitic ODS steels.

Addition of Hf and Zr increases hardness from 260 Hv to 340 Hv as shown in Fig. 6. Susila[2] , *et al*. have theoretically calculated the contributions of overall strength of ODS steel and base material from each strengthening mechanism and compared with experimental values.

6. VOID SWELLING

The term void swelling is defined as the increase in volume of metals, which are exposed to high dosage of neutron environment. Neutron irradiation leads to the displacement of atoms from their lattice positions, thus tends to form the vacancies-interstitial pairs. At high temperatures these vacancies become mobile and result in the formation of voids. These voids combine with helium atoms during the nuclear reaction and cause instability to the material which is known as helium embrittlement. The dimensional changes produced by void swelling cause damage to the material[17].

Austenitic stainless steel is highly prone to void swelling due to its crystal structure. It has been widely reported that the

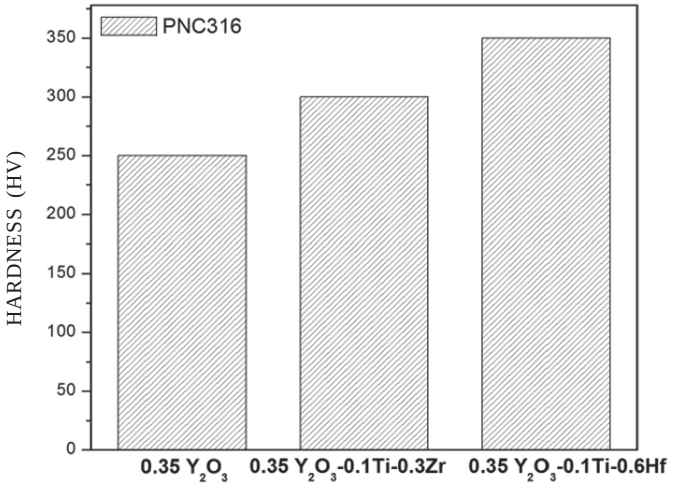

Figure 6. Effect of Zr and Hf on hardness of PNC316 alloy (replotted from[14]).

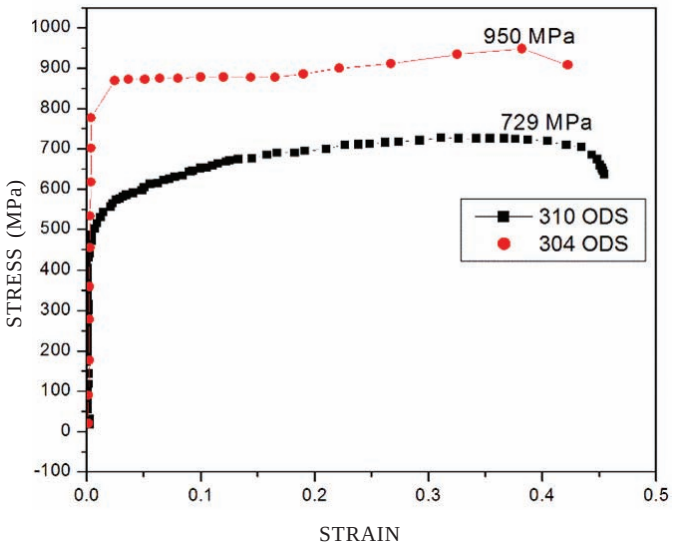

Figure 7. *In-situ* tensile behaviour of 310 and 304 ODS alloys (replotted from[4,11]).

dispersion of nano-sized oxide particles in austenitic steels can improve swelling resistance and high radiation doses. Compared to ferritic ODS steels, austenitic ODS steels generally possess better mechanical strength, creep and corrosion resistance at elevated temperatures. The interface between the oxide particle and matrix can act as sink for vacancies and it avoids void swelling. The electron irradiation has been carried out to measure irradiation resistance of the austenitic ODS steels. The amount of irradiation is measured in terms of displacement per atom (dpa).

There are two modes to carry in-situ TEM irradiation testing which are weak beam dark field (WBDF) and two-beam bright field (TBF) techniques. The samples are irradiated at 0.5 dpa to 15 dpa with and without helium implantation. The operating temperature during irradiation ranges from 400 °C - 500 °C. The helium implantation rates varies from 20 appm/dpa - 200 appm/dpa. Irradiation studies are carried out in PNC316 and ODS 316.

The microstructure of PNC316 and ODS316 steels shows very low initial dislocation density. Irradiation causes variation in microstructure and dislocation loops are formed in interface between the oxide particle and matrix. Faceted cavities are formed in both PNC316 and ODS316 alloys but in ODS316 cavities are formed at interface. High vacancy concentration and high dislocation loop formation are major contribution of nucleation of cavities at interface. Distribution of oxide particles has to be optimum so that mean free path of vacancy is not greater than the distance between the oxides.After the irradiation, ODS316 steels shows void swelling less than 0.2 per cent. The helium implantation increases the rate of void swelling and it tends to form coarse precipitates. Helium atoms act as nucleation sites of cavities[18]. Zhang[12], *et al*. have also reported the instability of phases due to irradiation. The large precipitates are stable upto 8 dpa. After 2.5 dpa, precipitation of $M_{23}C_6$ particles was confirmed using diffraction pattern. The irradiation induced precipitates preferentially nucleate along the grain boundaries at 2.5 dpa. At 5 dpa, more precipitates were formed within the grain interior and coarsening can be observed. Figure 8 shows the cavity evolution in ODS316 and PNC316 austenitic steel. It clearly shows that in PNC316 steels the faceted cavity structure evolves. In ODS316, the cavities evolve at matrix and cluster interface. The interface between oxide and matrix act as sink for cavities in ODS316 alloy[18].

7. SUMMARY

Austenitic steels with Y_2O_3 and Ti dispersoids and their processing methods are summarised. The influence of various process parameters on the nature, size, number density and morphology of dispersoids are discussed in detail. Most of austenitic ODS steels show better high temperature properties and irradiation resistance than ferritic ODS steels. Y-Ti-O clusters are widely reported with size range from 10 nm - 100 nm. These clusters help in improving the mechanical property due to complex interaction of dislocation and dispersoids. The tensile and yield strength show significant increase in the austenitic ODS steels than austenitic steels. But the ductility appears to decreased due to the formation of sigma phase. The presence of Ti helps in formation and uniform distribution

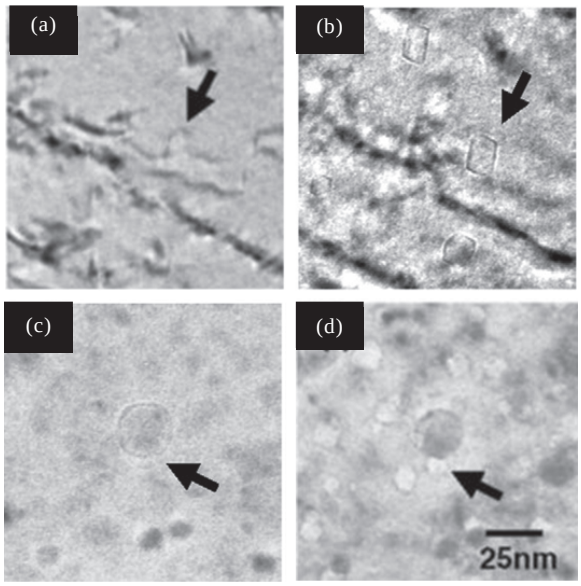

Figure 8. Cavity evolution in PNC316: (a) 7.6 dpa, (b) 12.7 dpa and ODS-316, (c) 3.3 dpa, and (d) 7.9 dpa irradiated at 823 K[18].

of the nanoclusters in the matrix. The influence of secondary mechanical processing after the synthesis of MA powders affects the properties. The secondary processing tends to increase the hardness of the material. The nanoclusters act as sink for vacancy and interstitials, thereby increasing the swelling resistance after irradiation. Electron irradiation, creep studies and hot deformation studies are some of fields having future endeavors in the field of austenitic ODS steels.

REFERENCES

1. Phaniraj, M.P.; Kim, D.I.; Shim, J.H. & Cho, Y.W. Microstructure development in mechanically alloyed yttria dispersed austenitic steels. *Acta Mater.*, 2009, **51**, 856–1864. doi: 10.1016/j.actamat.2008.12.026
2. Susila, P.; Sturm, D.; Heilmaier, M.; Murty B.S. & Sarma, V. Subramanya. Microstructural studies on nanocrystalline oxide dispersion strengthened austenitic (Fe-18Cr-8Ni-2W-0.25Y2O3) alloy synthesized by high energy ball milling and vacuum hot pressing. *J. Mater. Sci.*, 2010, **45**, 4858–4865. doi: 10.1007/s10853-010-4264-3
3. Kim, T.K.; Bae, C.S.; Kim, D.H.; Jang, J.; Kim, S.H.; Lee, C.B. & Hahn, D. Microstructural observation and tensile Isotropy of an austenitic ODS steel. *Nuclear Eng. Technol.*, 2008, 40, 4. doi: 10.5516/NET.2008.40.4.305
4. Miao, Y.; Mo, K.; Zhou, Z.; Liu, X.; Lan, K.; Zhang, G.; Miller, M.K.; Powers, K.A.; Almer, J. & Stubbins, J.F. In situ synchrotron tensile investigations on the phase responses within an oxide dispersion-strengthened (ODS) 304 steel. *Mater. Sci. Eng. A*, 2015, **625**, 146–152. doi: 10.1016/j.msea.2014.12.017
5. Wang, M.; Sun, H.; Zou, L.; Zhang, G.; Li, S. & Zhou, Z. Structural evolution of oxide dispersion strengthened austenitic powders during mechanical alloying and subsequent consolidation. *Powder Technol.*, 2015, **272**, 309–315. doi: 10.1016/j.powtec.2014.12.008
6. Xu, Y. & Zhou, Z. Processing and structure of a nitrogen alloyed oxide dispersion strengthened austenitic stainless steel by mechanical alloying. *J. Phys. Conf. Ser.*, 2013, **419**, 012052. doi: 10.1088/1742-6596/419/1/012052
7. Wang, M.; Zhou, Z.; Sun, H.; Hu, H. & Li, S. Microstructural observation and tensile properties of ODS-304 austenitic steel. *Mater. Sci. Eng. A*, 2013, **559**, 287–292. doi: 10.1016/j.msea.2012.08.099
8. Z. Zhou, S. Yang, W. Chen, L. Liao, and Y. Xu, Processing and characterization of a hipped oxide dispersion strengthened austenitic steel. *J. Nucl. Mater.*, 2012, **428**, 31–34. doi: 10.1016/j.jnucmat.2011.08.027
9. Xu, Y.; Zhou, Z.; Li. M. & He, P. Fabrication and characterization of ODS austenitic steels. *J. Nucl. Mater.*, 2011, **417**, 283–285. doi: 10.1016/j.jnucmat.2010.12.155
10. Wang, M.; Zhou, Z.; Sun, H.; Hu, H. & Li, S. Effects of plastic deformations on microstructure and mechanical properties of ODS-310 austenitic steel. *J. Nucl. Mater.*, 2012, **430**, 259–263. doi: 10.1016/j.jnucmat.2012.07.014
11. Miao, Y.; Mo, K.; Zhou, Z.; Liu, X.; Lan, K.; Zhang, G.; Miller, M.K. Powers, K.A.; Mei, Z.; Park, J.; Almer, J. & Stubbins, J.F. On the microstructure and strengthening mechanism in oxide disper- sion-strengthened 316 steel: A coordinated electron microscopy, atom probe tomography and in situ synchrotron tensile investigation. *Mater. Sci. Eng. A*, 2015, **639**, 585–596. doi: 10.1016/j.msea.2015.05.064
12. Zhang, H. K.; Yao, Z.; Zhou, Z.; Wang, M.; Kaitasov, O. & Daymond, M.R. Radiation induced microstructures in ODS 316 austenitic steel under dual-beam ions. *J. Nucl. Mater.*, 2014, **455**, 242–247. doi: 10.1016/j.jnucmat.2014.06.024
13. Koncz, P.; Horváth, Á.; Balázsi, K.; Şahin, F.Ç.; Göller, G.; Onüralp, Y. & Balázsi, C. Correlation between milling parameters, structural and mechanical properties of nanostructured austenitic Y2O3 strengthened steels. *Mater. Sci. Forum*, 2012, **729**, 409–414. doi: 10.4028/www.scientific.net/MSF.729.409
14. Oka, H.; Watanabe, M.; Ohnuki, S.; Hashimoto, N.; Yamashita, S. & Ohtsuka, S. Effects of milling process and alloying additions on oxide particle dispersion in austenitic stainless steel. *J. Nucl. Mater.*, 2014, **447**, 248–253. doi: 10.1016/j.jnucmat.2014.01.025
15. Miao, Y.; Mo, K.; Cui, B.; Chen, W. Y.; Miller, M.K.; Powers, K.A.; McCreary, V.; Gross, D.; Almer, J.; Robertson, I.M. & Stubbins, J.F. The interfacial orientation relationship of oxide nanoparticles in a hafnium-containing oxide dispersion-strengthened austenitic stainless steel. *Mater. Charact.*, 2015, **101**, 136–143. doi: 10.1016/j.matchar.2015.01.015
16. Oka, H.; Watanabe, M.; Hashimoto, N.; Ohnuki, S.;

Yamashita, S. & Ohtsuka, S. Morphology of oxide particles in ODS austenitic stainless steel. *J. Nucl. Mater.*, 2013, **442**, 164–168.
doi: 10.1016/j.jnucmat.2013.04.073

17. David, C.; Panigrahi, B. K.; Balaji, S.; Balamurugan, A.K.; Nair, K.G.M.; Amarendra, G. & Sundar, C.S. A study of the effect of titanium on the void swelling behavior of D9 steels by ion beam simulation. *J. Nucl. Mater.*, 2008, **383**, 132–136.
doi: 10.1016/j.jnucmat.2008.08.049
18. Oka, H.; Watanabe, M.; Kinoshita, H.; Shibayama, T.; Hashimoto, N.; Ohnuki, S.; Yamashita, S. & Ohtsuka, S. In-situ observation of damage structure in ODS austenitic steel during electron irradiation. *J. Nucl. Mater.*, 2011, **417**, 279–282.
doi: 10.1016/j.jnucmat.2010.12.156

CONTRIBUTORS

Ms Lavanya Raman is currently pursuing his PhD in the Department of Metallurgical and Materials Engineering, Indian Institute of Technology Madras, Chennai.

Mr Karthick Gothandapani is currently pursuing his PhD in the Department of Metallurgical and Materials Engineering, Indian Institute of Technology Madras, Chennai.

Prof. (Dr) B.S. Murty is currently working as Professor and Head, Department of Metallurgical and Materials Engineering, Indian Institute of Technology Madras, Chennai. His current area expertise include: High entropy alloys, nano materials, oxide dispersion strengthened steels, bulk metallic glasses.
In the current study, all the three authors have contributed equally in the manuscript preparation and writing.